J Biomol NMR (2013) 57:155–166
DOI 10.1007/s10858-013-9776-0

ARTICLE

Practical considerations over spectral quality in solid state NMR spectroscopy of soluble proteins

Marco Fragai · Claudio Luchinat · Giacomo Parigi · Enrico Ravera

Received: 29 June 2013 / Accepted: 23 August 2013 / Published online: 30 August 2013
© Springer Science+Business Media Dordrecht 2013

Abstract Great theoretical and methodological advances are pushing the limits of resolution and sensitivity in solid state NMR (SSNMR). However, sample preparation remains a critical issue for the success of an experiment. The factors affecting spectral quality in SSNMR samples are discussed, examining cases encountered in the literature and presenting new experimental data. A discussion on resolution and sensitivity in sedimented solutes is framed in this context.

Keywords Ultracentrifuge · Sedimentation · Solid state NMR · Sample preparation · Frozen solution · Cryoprotection · Ubiquitin · Superoxide dismutase

Introduction

Solid state NMR (SSNMR) has seen an outstanding theoretical and experimental development in the last years, which is bringing it to compete with state of the art solution NMR. Besides the samples that can be studied at atomic resolution only by SSNMR such as fibrils, membrane proteins and large protein aggregates (Bertini et al. 2011a; Tycko 2011; Paravastu et al. 2008; Qiang et al. 2012; Petkova et al. 2002; Wasmer et al. 2008; Lv et al. 2012; Van der Wel et al. 2007; Debelouchina et al. 2010; Lewandowski et al. 2011c; Bayro et al. 2011; McDermott 2009; Akbey et al. 2010b; Hefke et al. 2011; Murray et al. 2013; Loquet et al. 2010, 2012, 2013; Yan et al. 2013), crystalline preparations have been also extensively investigated through this technique (Knight et al. 2011, 2012a, b, 2013; Luchinat et al. 2012; Sengupta et al. 2013; Bertini et al. 2010; Balayssac et al. 2007). Crystalline proteins, similar to those used for X-ray diffraction (Martin and Zilm 2003; Keniry et al. 1983; Rothgeb and Oldfield 1981; Cross and Opella 1983; Smith et al. 1989; Cole and Torchia 1991; McDermott et al. 2000), usually yield high resolution spectra and are commonly used as a benchmark for developing new SSNMR methods (Franks et al. 2012), like pulse sequences (Laage et al. 2008, 2009a, b; Webber et al. 2012; Barbet-Massin et al. 2013; Salager et al. 2009; Lewandowski et al. 2010, 2011b; Turano et al. 2010) and specific selective labeling schemes (Castellani et al. 2002; Knight et al. 2011; Asami et al. 2012; Lewandowski et al. 2011a).

Crystals are not the ideal-suited target for biomolecular SSNMR: if they are formed, X-ray diffraction yield more easily structures at higher resolution. Furthermore, it is common experience of structural biologists that obtaining crystals may not be always straightforward, see for example (Benvenuti and Mangani 2007). For this reason, simpler approaches are sought for. For instance, SSNMR on frozen protein solutions has been applied for the investigation of protein folding, dynamical disorder (Havlin and Tycko 2005; Hu et al. 2010), and of soluble proteins that are too big for liquid-state NMR spectroscopy. Low temperatures can be used to increase the signal-to-noise ratio by increasing the Boltzmann population of the lowest energy state (Allen et al. 1991; Thurber and Tycko 2008; Tycko

Electronic supplementary material The online version of this article (doi:10.1007/s10858-013-9776-0) contains supplementary material, which is available to authorized users.

M. Fragai · C. Luchinat (✉) · G. Parigi · E. Ravera
Center for Magnetic Resonance (CERM), University of Florence, Via L. Sacconi 6, 50019 Sesto Fiorentino, FI, Italy
e-mail: claudioluchinat@cerm.unifi.it

M. Fragai · C. Luchinat · G. Parigi · E. Ravera
Department of Chemistry, University of Florence, Via della Lastruccia 3, 50019 Sesto Fiorentino, FI, Italy

2013; Concistre et al. 2013), also in combination with dynamic nuclear polarization (DNP) (Barnes et al. 2009; Van der Wel et al. 2006; Hall et al. 1997; Akbey et al. 2010a; Ni et al. 2013; Corzilius et al. 2012; Corzilius et al. 2011; Barnes et al. 2009; Matsuki et al. 2009; Hu et al. 2004, 2007; Weis and Griffin 2006). Most of the biomolecular DNP studies reported to date rely on frozen glycerol-water solutions, because glycerol serves as cryoprotectant and prevents ice formation and subsequent formation of separate (bi)radical grains (Barnes et al. 2008). However the price of this intrinsic simplicity is an increased linewidth that can become a prohibitive limiting factor (Siemer et al. 2012).

Freeze-drying has also been extensively applied in the pioneering studies in protein SSNMR spectroscopy (Harbison et al. 1985; Huang et al. 1984; Auger et al. 1993). However, lyophilized samples usually suffer from line broadening more than frozen solutions, even if lyoprotecting molecules are added to the solution prior to lyophilization (Jakeman et al. 1998; Pauli et al. 2000). This is likely due to the complete loss of the protein hydration layer, which is expected to play an "averaging" role (Martin and Zilm 2003; Linden et al. 2011) (see also later).

In 2009 Mainz et al. proposed that the increase in solution viscosity due to glycerol, in conjunction with high concentrations and low temperatures, could prevent rotational diffusion and provide solid state spectra for large protein complexes. Solid state spectra of αB-crystallin were indeed observed under these conditions (Mainz et al. 2009). However, high viscosity, high concentrations and low temperatures are not enough to abolish rotational diffusion on the SSNMR relevant timescale (i.e., ≫microseconds) for proteins up to about 1 MDa mass, as it was later shown (Ravera et al. 2013b). The 2009 observation was given a different explanation in 2011 (Bertini et al. 2011b), when it could be shown that rotational diffusion is actually quenched by sedimentation in the MAS rotor. Since then, the idea of NMR of sedimented solutes (Sed-NMR) was introduced as an alternative way to prepare samples for SSNMR (Bertini et al. 2011b, 2012b, 2013, b). It was demonstrated that the particle packing achieved by ultracentrifugation is sufficient to prevent rotational motions, thus allowing for detection of SSNMR signals. The spectra collected for a number of different systems indicate that spectral resolution in sediments is rather high, comparable to that of crystals (Bertini et al. 2012b; Gardiennet et al. 2012; Mainz et al. 2012; Baldwin et al. 2012). Here we present some considerations on the effects that make the spectral quality of sediments comparable to that of microcrystalline preparations with extremely simplified sample manipulation. We also show that proteins as small as 32 kDa can be efficiently sedimented in a MAS rotor, and proteins as small as ubiquitin (8.6 kDa in the monomeric form, 17 kDa in the dimeric high concentration conditions (Liu et al. 2012)) can be sedimented with ultracentrifugal devices and studied as solids with sufficient signal-to-noise ratio.

Effect of hydration and freezing on resolution in crystalline preparations

X-ray crystallography and SSNMR have different sample requirements: X-ray crystallography requires 20–30 μm crystals [only rarely powder diffraction allows for structural reconstruction (Margiolaki et al. 2007)]; crystals for SSNMR have no size requirements, as long as crystal order is present (Martin and Zilm 2003; Gardiennet et al. 2012), such as in powder preparations referred to as nanocrystals or "precipitates". Crystals for X-ray diffraction are usually soaked in a cryoprotectant, because freezing at liquid nitrogen temperature is required for preventing radiation damage. Conversely, cryogenic temperatures are usually avoided in SSNMR because low temperatures are detrimental for the resolution. The explanation often invoked for NMR line broadening at cryogenic temperatures is that also the protein-bound solvent molecules are frozen, and upon immobilization of protein-bound solvent molecules, there is heterogeneity in the environment around the solvent-exposed surfaces of equivalent protein molecules (Martin and Zilm 2003; Linden et al. 2011; Siemer and McDermott 2008). In this assumption, freezing of bulk water without freezing of the protein-bound water molecules should not affect the spectral resolution to an appreciable extent (Linden et al. 2011), as experimentally verified for a number of proteins (Martin and Zilm 2003; Linden et al. 2011; Siemer and McDermott 2008).

Perturbation of the protein hydration layer (e.g. by freezing or drying) has a profound impact on the spectral resolution of crystalline samples, as extensively discussed in Igumenova et al. (2004a, b). In order to exemplify such effect, we have monitored the effect of protein dehydration/rehydration by performing the following experiments on microcrystalline ubiquitin packed in a Bruker 3.2 rotor with a standard cap. After overnight spinning at 14 kHz and 269 K (effective sample temperature), the NMR spectrum showed severe broadening of the resonances. After addition of 8 μl of the mother liquor, the spectral quality reverted to the starting one (Fig. 1). By sealing the sample using a silicon soft plug (Bruker Biospin), the dehydration problem is mitigated and the spectral quality is preserved over a longer time. This confirms that hydration is necessary to preserve spectral quality over the experimental time, and that great care must be applied in the sample handling, so that no dehydration can occur. The use of silicon sealings, or anyway airtight rotors, is in principle the best way to achieve this result.

Protein sediments for SSNMR

In a sediment 50 % or more of the sample is composed of protein (Lundh 1980, 1985). Bearing this in mind, one can expect this extreme proximity between protein molecules to sizably affect their properties, as evidenced by the following experiments:

1. The frozen protein sediment prepared by spinning an aqueous solution directly in the MAS rotor is suitable to disperse (bi)radicals for DNP, suggesting that the close proximity of protein molecules prevents the biradical segregation that would occur if ice crystals were formed. This indicates that the frozen sediment is not as susceptible to ice formation within the bulk solvent as is a homogenous frozen solution (Ravera et al. 2013a), Fig. 2;
2. The reorientation motions of the protein molecules are largely suppressed by the tight packing of the molecules: field-dependent relaxation profiles are closer (Luchinat et al. 2013) to those of the lyophilized proteins (Diakova et al. 2010), than to those of proteins when free in solution (Ravera et al. 2013b).

Thus, sediments are hydrated and solid on the NMR-relevant timescales, and tight packing prevents bulk ice-protein interactions. These properties provide a simple explanation of the high quality of the SedNMR spectra reported so far.

To delve further into the parameters affecting the resolution of SSNMR spectra of sediments, we examined two rather distinct protein systems: dimeric human superoxide dismutase (hSOD) and ubiquitin. hSOD was sedimented in situ, i.e.: using magic angle spinning of the rotor to create a gradient of protein concentration (Bertini et al. 2011b), while ubiquitin was sedimented ex situ (i.e.: outside the NMR instrument) (Bertini et al. 2012b), via an especially designed ultracentrifugal device to form and convey the sediment into the NMR rotor (Bertini et al. 2011b; 2012; Gardiennet et al. 2012; Gelis et al. 2013).

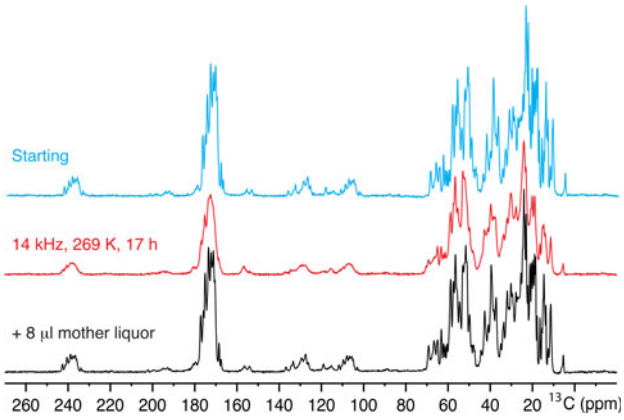

Fig. 1 ^{1}H–^{13}C CP spectra of microcrystalline ubiquitin (sample provided by Giotto Biotech), recorded at 20.0 T, 14 kHz MAS, 269 K. In *cyan* the spectrum recorded at the beginning of the experiment, in red the spectrum after 17 h spinning, in *black* the spectrum after rehydration of the sample with 8 µl of the mother liquor and sealed with a soft plug (Bruker Biospin)

Materials and methods

Isotopically enriched ^{13}C–^{15}N ubiquitin and a C6A/C111S doubly mutated human superoxide dismutase (hSOD) were purchased from Giottobiotech (www.giottobiotech.com) and used without further purification. Spectra of crystalline ubiquitin were kindly provided by Giottobiotech. Crystallization conditions were those reported in Igumenova et al. (2004a).

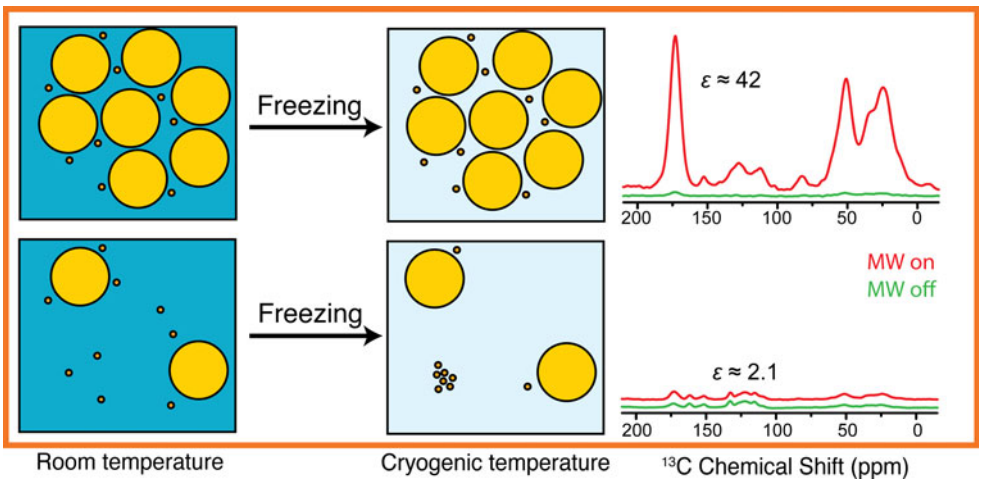

Fig. 2 DNP enhanced ^{1}H-^{13}C CP spectra of frozen sediment (*top*) and frozen solution (*bottom*) of the 24-meric protein apoferritin [adapted with permission from (Ravera et al. 2013a)]. The effect of segregation of radicals (*small circles*) in the latter case is evident in the reduced DNP effect

Ultracentrifugal device

Packing of crystalline ubiquitin and ex situ sedimentation of ubiquitin in MAS rotors were carried out using an ultracentrifugal device, supplied by Giottobiotech. The device has been extensively described in (Bertini et al. 2012a) and therein referred to as "device 2". The inner volume of the device is 1.36 ml; the total volume over the volume of the MAS rotor amounts to 85 times. This ratio is much more than needed, given that ubiquitin can be easily concentrated up to 100 mg/ml. In case the attainable protein concentrations were lower, the "device 1" (Bertini et al. 2012a) should rather be used, with a inner volume of 23 ml, i.e.: a total volume/rotor volume ratio of 1,437, which is a factor 17 larger than for the "device 2" (Bertini et al. 2012a) and 6 times larger than for the device described by (Gelis et al. 2013).

The relevant equations to calculate the amount of sediment that is formed within the rotor volume are given in (Bertini et al. 2012a).

In situ sedimentation

hSOD was concentrated to 200 mg/ml. 16.4 µl of concentrated protein solution were transferred into a Bruker 3.2 mm rotor and spun on a tabletop spinner to remove air bubbles, that easily form at high protein concentration. Bubbles removal is critical for rotation stability and shimming. The rotor was sealed with a DNP silicon plug (Bruker biospin) to avoid leakage.

Ex situ sedimentation

Ubiquitin was concentrated to 100 mg/ml and transferred into the ultracentrifugal device. The ultracentrifugation was carried out using a Beckman Coulter L80K floor preparative ultracentrifuge equipped with a SW32 rotor. The device (40 g) was balanced with a sucrose solution. The rotation speed was set to 32,000 rpm and the ultracentrifugation was run over 6 days. This is longer than the time that a single ubiquitin molecule (sedimentation coefficient 1.14 S, calculated with hydropro (de la Torre et al. 2000)) would need to travel from the meniscus to the bottom of the device (the clearing factor of the rotor equipped with the device is $k = 128.9$) according to the Svedberg equation. However, since at high concentration ubiquitin tends to form a non covalent dimer (Liu et al. 2012), the sedimentation efficiency is expected to be higher (sedimentation coefficient for covalent ubiquitin dimer is 1.69 S (Ivins et al. 2009)). The sample was then closed without sealing. By weighting the sample before and after several days of spectra acquisition no weight loss was observed, and thus no sealing was actually required in this case.

SSNMR spectra were recorded on Bruker AvanceII spectrometers operating at 700 MHz (16.4 T) or 850 MHz (20 T) proton Larmor frequency. Experimental conditions are given along with the spectra. Temperature calibration was performed based on ^{79}Br chemical shift, with temperature sensor reading between 227 and 300 K (Thurber and Tycko 2009).

Field dependent NMRD profiles were acquired over the 0.01–40 MHz range with a Stelar Spinmaster FFC relaxometer. Profiles were fitted to the sum of three Lorentzian functions as described in (Ravera et al. 2013b).

Results

Sedimentation of human superoxide dismutase

The 32 kDa dimeric protein hSOD was sedimented in situ in a Bruker 3.2 mm rotor from a 200 mg/ml solution. SSNMR spectra were collected at 20 T and 290.8 K (see Fig. 3). As observed in other in situ sedimentation experiments (Bertini et al. 2011b, 2013a), the sample becomes responsive to dipolar-based cross-polarization (CP) experiments (Pines et al. 1972) upon spinning. The solid state like signal appears after several hours of MAS [consistent with what predictable from the sedimentation coefficient of the dimeric hSOD (Doucette et al. 2004)], and it disappears after MAS is stopped, thus indicating that no aggregation is occurring. In fact, if the protein would have formed aggregates, sedimentation should have occurred much faster. Fully oxidized and fully metallated hSOD is actually known to be extremely stable as a dimer (Sheng et al. 2012) and does not show any evidence of aggregation (Banci et al. 2007, 2008), especially in the mutant C6A/C111S form: the removal of these two cysteines that are not involved in intramolecular disulfide bonds brings the protein close to the bovine protein, which is stable as a dimer up to 8 mM concentrations (Banci et al. 1990).

The quality of the spectra for sedimented hSOD is very high, with lines as sharp as 80 Hz (i.e.: the linewidth reflects the ^{13}C–^{13}C J-couplings, as the acquisition time is too short to allow for resolution of the signal components; longer acquisition times are prevented by instrumental limitations). It was reported that the freezing of the solvent does not affect the quality of the SSNMR spectra of protein sediments as much as of protein solutions (Ravera et al. 2013a), so that no sizable change in the spectral quality is expected for a sediment above and below the freezing of bulk water. This is actually verified for the sedimented hSOD, as shown in Fig. 4.

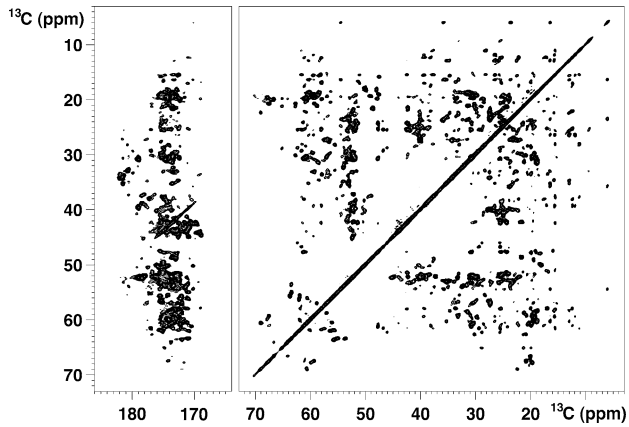

Fig. 3 DARR spectrum of hSOD sedimented in situ, recorded at 20.0 T, 14 kHz MAS, 290.8 K effective sample temperature

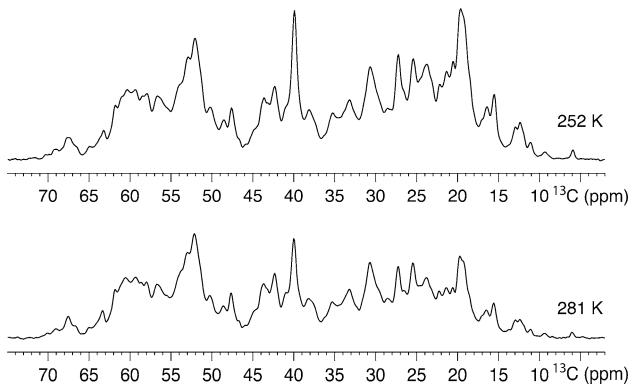

Fig. 4 ^{1}H–^{13}C CP spectra of hSOD sedimented in situ, recorded at 16.4 T, 14 kHz MAS, at 252 K (*top*) and 281 K (*bottom*)

We notice that hSOD is the first example of a small protein providing highly resolved spectra for a sample sedimented in situ.

Sedimentation of ubiquitin

Ubiquitin (8.6 kDa) was sedimented ex situ into a Bruker 3.2 mm rotor using the device and the procedure described in the "Materials and methods" section (Bertini et al. 2012a). The procedure resulted in 21 mg of protein sediment packed into the 3.2 mm SSNMR rotor (inner volume 16.3 µl). The protein in the sediment obtained in this way had a concentration of 847 mg/ml.[1] Such extremely high concentration is likely achieved because of the low charge of ubiquitin at pH 7.5 (as can be calculated from the protein

[1] This value is calculated by comparing the Direct Polarization signal intensity of the present sample to the same spectrum of a sample comprising of 6 mg of lyophilized ubiquitin, rehydrated to 400 mg/ml with a glycerol/water mixture. A concentration value of 833 mg/ml can be calculated under the assumption that conc = $(\rho_{sol} - \rho_{solv})/(1 - \rho_{solv}/\rho_{prot})$ (Chatelier and Minton 1987).

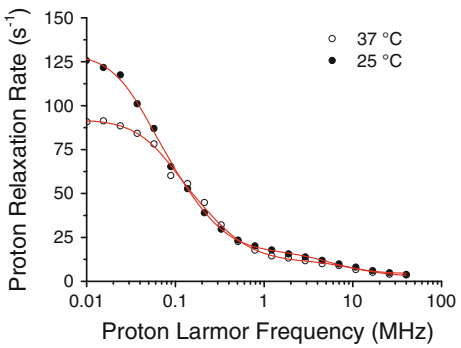

Fig. 5 NMRD profiles of sedimented ubiquitin recorded at 37 and 25 °C. The profiles were fitted to a sum of Lorentzians

sequence). From the crystal cell parameters available in the PDB deposition 3ONS (Huang et al. 2011), it can be estimated that ubiquitin crystals have a protein concentration of 734 mg/ml. With these data at hand, the NMR signals of the sedimented ubiquitin sample are expected to provide a signal-to-noise ratio similar or slightly smaller than that of the nanocrystalline preparation. Conversely, by comparison of the direct polarization spectra (DP), this ratio was experimentally found to be 1.45 times larger for the sedimented sample than for the crystal sample. As further discussed in the next section, this discrepancy can be ascribed to the different packing efficiency during sample preparation, despite the use of the same packing device (Bertini et al. 2012a).

As for the hSOD sample, also the sedimented ubiquitin is responsive to CP. However, at room temperature, the CP signal is about 25 % of the DP signal, and the linewidths are rather large. This suggests that the ubiquitin sediment, at variance with the hSOD sample, is not packed tightly enough to completely abolish motions on the SSNMR relevant timescale (i.e.: in times much larger than microseconds, for MAS rates of tens of kHz).

By fast-field-cycling relaxometry, the spectral density for the dipole–dipole interactions of the ubiquitin sediment can be directly measured, as described in (Venu et al. 1997; Denisov et al. 1997; Kiihne and Bryant 2000; Hills 1992; Bertini et al. 2001; Libralesso et al. 2005; Ravera et al. 2013b). The field-dependent relaxation profiles (see Fig. 5) show a low-field dispersion typical of large proteins but not the power-low dependence typical of lyophilized proteins and of well-formed sediments (Luchinat et al. 2013; Goddard et al. 2009). Fitting of the NMRD profiles acquired at 310 and 298 K resulted in a correlation time at 298 K of 1.8 µs. This value is more than two orders of magnitude longer than the value of 4.1 ns observed for the rotational correlation time of free ubiquitin (Lee and Wand 1999), but still too fast to consider the molecule immobile over one (or more) MAS rotor period. Therefore, this

finding explains the inability of sedimented ubiquitin to properly respond to CP as a well-formed sediment should.

However, an abrupt change in the appearance of the SSNMR spectra of sedimented ubiquitin occurs just below the freezing temperature of the bulk water: the overall intensity of the CP signal dramatically increases, and the lines become relatively sharp (Fig. 6). The relative intensity of the CP signal as a function of temperature is reported in Fig. 7.

It is important to notice that all protein sediments published so far, as well as the hSOD sediment in the present work, showed highly resolved spectra also before solvent freezing. This different behavior of ubiquitin is likely due to the small protein size.

The signal in the frozen sediment is dramatically increased, by more than a factor 3. It reaches a magnitude of about 1.2 times the direct polarization signal, a value that is not far from the about 1.4 magnitude ratio observed for crystals. After rescaling of the intensity, the cross polarization dynamics in the frozen sediment and in the crystalline sample is superimposable, as shown in Fig. 8.

It is worth noting that, under the employed conditions (MAS = 14 kHz, T = 269 K), the experiments indicate that sediments are less prone to dehydration than microcrystals. In fact, while the microcrystalline ubiquitin sample undergoes dehydration without proper sealing (Fig. 1), the same does not hold for the sediment.

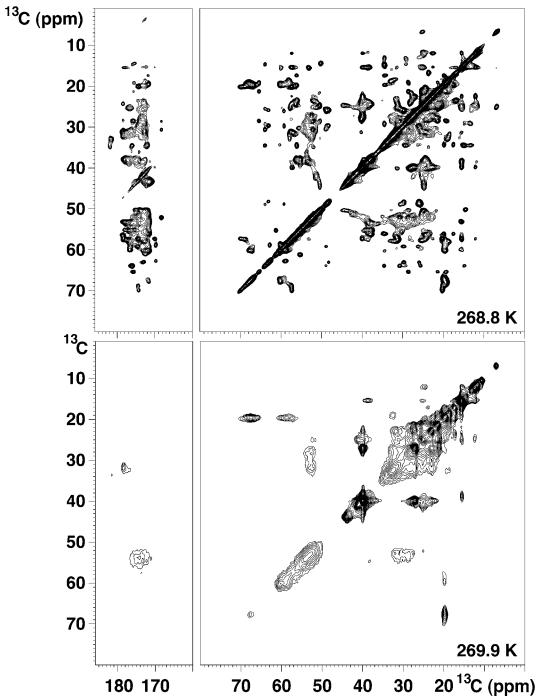

Fig. 6 Comparison of the DARR spectra of ex situ sedimented ubiquitin, recorded at 850 MHz ^{1}H Larmor frequency, 14 kHz MAS, 100 kHz ^{1}H SWTTPM 1H decoupling, around the freezing of the bulk solvent. *Top* 268.8 ± 0.4 K, *bottom* 269.9 ± 0.7 K

From the sample preparation viewpoint, the frozen sediment sample should be similar to the frozen solutions that are sometimes employed in SSNMR. It is widely known that freezing is the cause of severe line broadening in such samples. Siemer et al. (Siemer et al. 2012) suggested that the sharpest lines in frozen solution NMR are observed at the freezing temperature of the bulk. In agreement with the measurements on ubiquitin frozen solutions reported in (Siemer et al. 2012), a linewidth of the order of 120 Hz is observed in the present case of frozen sedimented ubiquitin. The spectral resolution is in this case

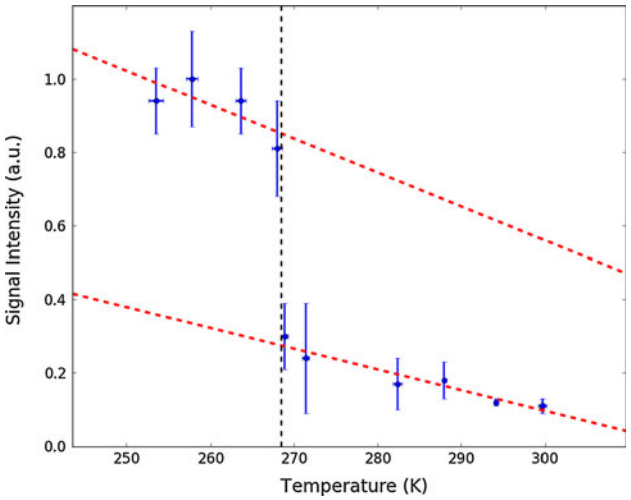

Fig. 7 Temperature dependence of the ^{1}H–^{13}C CP signal of carbonyls in sedimented ubiquitin. Linear regressions are only provided as a guide to the eyes. The *black vertical dashed line* indicates the estimated freezing point

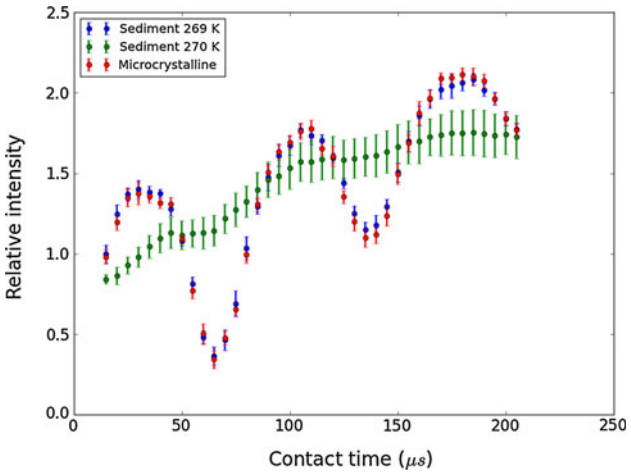

Fig. 8 ^{1}H–^{13}C$^{\alpha}$ cross polarization dynamics for ubiquitin frozen sediment and microcrystals, recorded at 850 MHz ^{1}H Larmor frequency, 14 kHz MAS. Essentially the same degree of immobilization is observed for the frozen sediment and microcrystals, while the difference with the sediment before the freezing of the bulk solvent (in *green*) is apparent

lower than that of the microcrystalline preparation, with linewidth around 80 Hz (see Fig. 1). SSNMR spectra are also available for lyophilized ubiquitin (6 mg) hydrated with H_2O (10 μL) after lyophilization (Seidel et al. 2005). The high quality of these spectra strongly suggests that a rehydrated lyophilized material corresponds directly either to a sediment or to an extremely concentrated solution that easily forms a sediment under MAS (Bertini et al. 2013b).

However, there are significant conceptual differences between sedimented samples and solutions, as seen from the temperature dependence of the ubiquitin samples:

1. a CP spectrum of sedimented ubiquitin, as opposed to the solution, can be observed also above the freezing point of the bulk solvent, although it appears rather broad because of the incomplete immobilization, as summarized in Fig. 5;
2. above the freezing temperature, the DP spectrum of sedimented ubiquitin has much larger linewidth than the DP spectrum of the ubiquitin solution presented in Fig. 1 in Siemer et al. (2012), indicating that protein crowding in the sediment is increasing the reorientational correlation time (as also indicated by the NMRD profiles), with a consequent line broadening.

Discussion

Can sedimentation be even more efficient than crystallization for SSNMR sample preparation? In the following, we will try to address this question through examples and theoretical calculations.

In crystals, protein volume fractions are in the 19–80 % range (Kantardjieff and Rupp 2003): averaging around 56.5 % (Andersson and Hovmoller 2000).

The variety in protein volume fraction of sediments could be expected to be as large as in crystals: highly charged molecules tend to have larger effective volumes than neutral molecules of the same size (Minton 2007), resulting in volume fractions as low as 15 % (Rivas and Minton 2011) while for the less charged molecules, values up to 62 % have been reported and in favorable cases the theoretical limit of the close packing of rigid spheres of 74 % (or even beyond for non spherical particles) could in principle be approached.

The relative packing efficiency between crystallization and ex situ sedimentation strongly depends on the nature of the macromolecule. For instance, the ex-situ sediment of the 24-meric bullfrog apoferritin was found to give a 128-fold enhanced signal-to-noise ratio with respect to the in situ sediment obtained at 60 mg/ml (Bertini et al. 2012b). This translates into 670 mg/ml concentration. Conversely, apoferritin crystals are found to have a very high solvent content (71 %) (Ha et al. 1999), resulting in 391 mg/ml concentration. In this case, even assuming a perfect packing of the crystals in the rotor, the signal of the sediment should be almost twice as intense.

On the contrary, the concentration in the ex situ sediment of the dodecameric helicase DNAb was found to be roughly half of that in the corresponding microcrystalline preparation, and estimated to 200 mg/ml (Gardiennet et al. 2012). As already mentioned, a high protein charge leads to sediments with low protein concentrations (Chatelier and Minton 1987). Therefore, for helicase DNAb, this value at the low end of the concentration range found in sediments is likely to reflect the high charge of the molecule.

The abovementioned examples are reporters of the large variety that can be expected for protein sediments. It is instructive to compare the limiting volume fractions that are observed in the protein sediments reported so far with the crystalline preparations of the same proteins. The data are reported in Table S1 and Fig. 9. It appears that some proteins can be more concentrated in sediments than in crystals, although in many cases their concentration is similar. Nevertheless, even proteins that are expected to achieve about the same volume fraction in the two preparations may display a larger signal-to-noise ratio in sedimented samples than in crystalline samples, as in the case of ubiquitin, due to the more efficient packing in the sediment than in the microcrystalline sample preparation. In fact, packing a rotor with a microcrystalline preparation may result in a large intercrystallite void volume. This problem can be mitigated by the use of rotor-filling tools for ultracentrifuge (Böckmann et al. 2009). Conversely, in

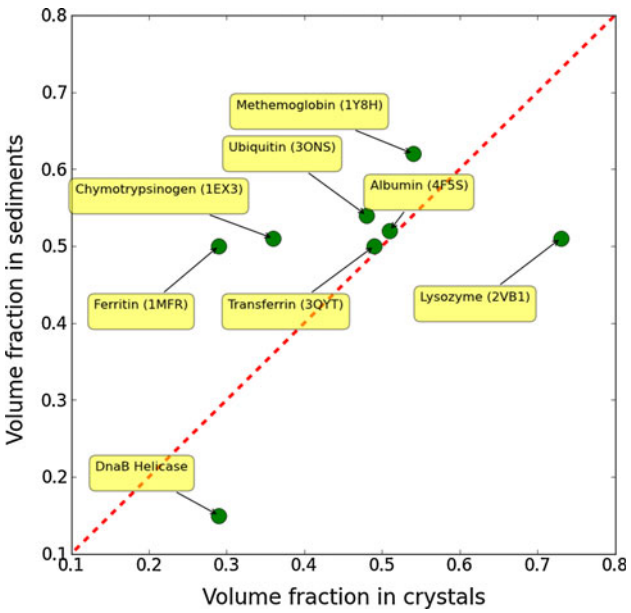

Fig. 9 Comparison of protein volume fractions in sediments and in crystals

the case of ex situ sedimentation, no void volume at all is present in the rotor.

The efficient packing of the investigated molecules that can result through sedimentation represents a clear advantage of this technique for SSNMR sample preparation. This advantage should be considered together with the ease in the preparation of the sediment samples.

In situ sedimentation represents a versatile and quick approach to SSNMR sample preparation, and can also be regarded as a quick way to check a sample before going into large scale protein production. Here we have demonstrated that it can be easily applied to proteins as small as 32 kDa. When the protein size is even smaller, as in the case of ubiquitin, or sensitivity is an issue, one can resort to ex situ sample preparation. It has already been shown that ex situ sediment provides resolved spectra, and they yield excellent signal to noise ratio: the gain in sensitivity is large over the in situ preparation or over frozen solutions, as summarized in Fig. 10, because the rotor is fully packed with the protein sediment rather than with the protein solution. The advantage for a small protein is the following: if only a fraction of the protein can sediment at a given gravity, by ex situ sedimentation the rotor can be anyway filled: if, at a given MAS, 5 % of the protein is sedimented, only 5 % will be visible in the in situ experiment, while the rotor will be full of sediment in the ex situ experiment. However, a much larger amount of protein is required in this case: as noted in the Materials and Methods section, ex situ sedimentation is performed by the use of ultracentrifugal devices whose volumes are 100/1,000 times larger than the rotor. To ensure efficient sedimentation, the concentration of the protein solution should be anyway rather high. Thus a larger initial amount of protein is required.

To quantify the gain, one should consider that achieving protein volume fractions higher than 40 % in protein solutions can be technically demanding (Venturi et al. 2008), whereas the protein volume fraction in sedimented samples obtained from ultracentrifugation can reach a value of about 70 %, depending on the protein of interest. This allows for a sizable reduction of the experimental time. Ex situ sedimentation might also turn out to be more efficient than crystallization, given that the sediment tends to fill completely the rotor volume, while crystalline preparations always have intercrystallite void volume. This can be exemplified as follows: assuming, for simplicity, that the microcrystals are spheres containing perfectly packed spherical proteins, the maximum protein volume is $0.74 \times 0.74 = 0.55$, while for the sediment of the same protein it would be 0.74.

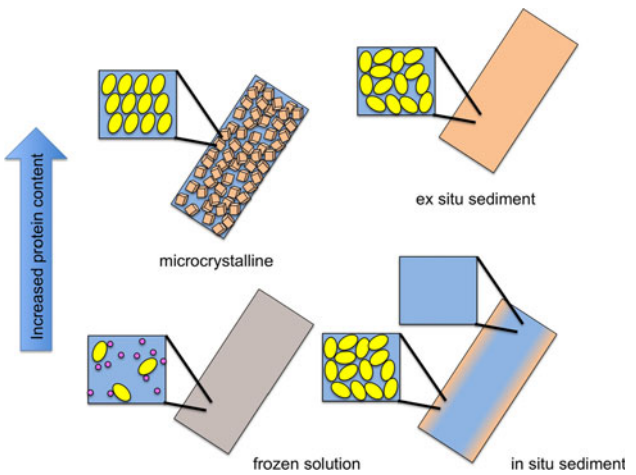

Fig. 10 Comparison of different SSNMR sample preparations for soluble proteins, ranked according to the overall protein amount

Conclusions

In this paper we have reviewed the observations over the linewidth of crystalline protein samples reported in the recent literature and we have framed in this context our considerations about the spectral quality of protein sediments, in term of resolution, signal intensity and stability over time. Ex situ sedimentation may also provide spectra of higher intensity (and resolution) than crystalline samples, if larger protein concentrations or increased packing efficiency are achieved in sediments than in crystals. We have shown that a small protein of 32 kDa can provide highly resolved in situ sediment spectra. In the case of even smaller proteins, the molecular packing in the sediment might not be enough to completely prevent rotational diffusion. Cooling the sediment just below the freezing of bulk solvent may yield again well resolved spectra, suitable for spectroscopic investigation. Practical guidelines for the various sample preparations are also given.

Acknowledgments Discussions with Lyndon Emsley, Moreno Lelli, Guido Pintacuda and Robert G. Griffin on resolution in SSNMR and with Vito Calderone on crystallization conditions are acknowledged. This work has been supported by Ente Cassa di Risparmio di Firenze, the European Commission (contract Bio-NMR no. 261863), and Instruct, part of the European Strategy Forum on Research Infrastructures (ESFRI) and supported by national member subscriptions. Specifically, we thank the EU ESFRI Instruct Core Centre CERM, Italy.

References

Akbey Ü, Franks T, Linden A, Lange S, Griffin RG, van Rossum B-J, Oschkinat H (2010a) Dynamic nuclear polarization of deuterated proteins. Angew Chem Int Ed 49:7803–7806

Akbey Ü, Lange S, Franks WT, Linser R, Rehbein K, Diehl A, van Rossum BJ, Reif B, Oschkinat H (2010b) Optimum levels of exchangeable protons in perdeuterated proteins for proton

detection in MAS solid-state NMR spectroscopy. J Biomol NMR 46:67–73
Allen PJ, Creuzet F, de Groot HJM, Griffin RG (1991) Apparatus for low-temperature magic-angle spinning NMR. J Magn Reson 92:614–617
Andersson KM, Hovmoller S (2000) The protein content in crystals and packing coefficients in different space groups. Acta Crystallogr D Biol Crystallogr 56:789–790
Asami S, Szekely K, Schanda P, Meier BH, Reif B (2012) Optimal degree of protonation for (1)H detection of aliphatic sites in randomly deuterated proteins as a function of the MAS frequency. J Biomol NMR 54:155–168
Auger M, McDermott AE, Robinson V, Castelhano AL, Billedeau RJ, Pliura DH, Krantz A, Griffin RG (1993) Solid-state carbon-13 NMR study of a transglutaminase-inhibitor adduct. Biochemistry 32:3930–3934
Balayssac S, Bertini I, Falber K, Fragai M, Jehle S, Lelli M, Luchinat C, Oschkinat H, Yeo KJ (2007) Solid-state NMR of matrix metalloproteinase 12: an approach complementary to solution NMR. ChemBioChem 8:486–489
Baldwin AJ, Walsh P, Hansen DF, Hilton GR, Benesch JLP, Sharpe S, Kay LE (2012) Probing dynamic conformations of the high-molecular-weight αB-crystallin heat shock protein ensemble by NMR spectroscopy. J Am Chem Soc 134:15343–15350
Banci L, Bencini A, Bertini I, Luchinat C, Piccioli M (1990) ^{1}H NOE and ligand field studies of copper-cobalt superoxide dismutase with anions. Inorg Chem 29:4867–4873
Banci L, Bertini I, Girotto S, Martinelli M, Vieru M, Whitelegge J, Durazo A, Valentine JS (2007) Metal-free SOD1 forms amyloid-like oligomers: a possible general mechanism for familial ALS. Proc Natl Acad Sci USA 104:11263–11267
Banci L, Bertini I, Boca M, Girotto S, Martinelli M, Valentine JS, Vieru M (2008) SOD1 and amyotrophic lateral sclerosis: mutations and oligomerization. PLoS One 3:e1677
Barbet-Massin E, Pell AJ, Knight MJ, Webber AL, Felli IC, Pierattelli R, Emsley L, Lesage A, Pintacuda G (2013) ^{13}C-detected through-bond correlation experiments for protein resonance assignment by ultra-fast MAS NMR. ChemPhysChem. doi:10.1002/cphc.201201097
Barnes AB, De Paëpe G, Van der Wel PCA, Hu K-N, Joo C-G, Bajaj VS, Mak-Jurkauskas ML, Sirigiri JR, Herzfeld J, Temkin RJ, Griffin RG (2008) High-field dynamic nuclear polarization for solid and solution biological NMR. Appl Magn Reson 34:237–263
Barnes AB, Mak-Jurkauskas ML, Matsuki Y, Bajaj VS, Van der Wel PCA, DeRocher R, Bryant J, Sirigiri JR, Temkin RJ, Lugtenburg J, Herzfeld J, Griffin RG (2009) Cryogenic sample exchange NMR probe for magic angle spinning dynamic nuclear polarization. J Magn Reson 198:261–270
Bayro MJ, Debelouchina GT, Eddy MT, Birkett NR, MacPhee CE, Rosay MM, Maas W, Dobson CM, Griffin RG (2011) Intermolecular structure determination of amyloid fibrils with magic-angle spinning and dynamic nuclear polarization NMR. J Am Chem Soc 133:13967–13974
Benvenuti M, Mangani S (2007) Crystallisation of soluble proteins in vapour diffusion for X-ray crystallography. Nat Protoc 2:1633–1651
Bertini I, Luchinat C, Parigi G (2001) Solution NMR of paramagnetic molecules. Elsevier, Amsterdam
Bertini I, Bhaumik A, De Paepe G, Griffin RG, Lelli M, Lewandowski JR, Luchinat C (2010) High-resolution solid-state NMR structure of a 17.6 kDa protein. J Am Chem Soc 132:1032–1040
Bertini I, Gonnelli L, Luchinat C, Mao J, Nesi A (2011a) A new structural model Aß40 fibrils. J Am Chem Soc 133:16013–16022
Bertini I, Luchinat C, Parigi G, Ravera E, Reif B, Turano P (2011b) Solid-state NMR of proteins sedimented by ultracentrifugation. Proc Natl Acad Sci USA 108:10396–10399
Bertini I, Engelke F, Gonnelli L, Knott B, Luchinat C, Osen D, Ravera E (2012a) On the use of ultracentrifugal devices for sedimented solute NMR. J Biomol NMR 54:123–127
Bertini I, Engelke F, Luchinat C, Parigi G, Ravera E, Rosa C, Turano P (2012b) NMR properties of sedimented solutes. Phys Chem Chem Phys 14:439–447
Bertini I, Gallo G, Korsak M, Luchinat C, Mao J, Ravera E (2013a) Formation kinetics and structural features of beta-amyloid aggregates by sedimented solute NMR. ChemBioChem. doi:10.1002/cbic.201300141
Bertini I, Luchinat C, Parigi G, Ravera E (2013b) SedNMR: on the edge between solution and solid state NMR. Acc Chem Res. doi:10.1021/ar300342f
Böckmann A, Gardiennet C, Verel R, Hunkeler A, Loquet A, Pintacuda G, Emsley L, Meier BH, Lesage A (2009) Characterization of different water pools in solid-state NMR protein samples. J Biomol NMR 45:319–327
Castellani F, van Rossum B, Diehl A, Schubert M, Rehbein K, Oschkinat H (2002) Structure of a protein determined by solid-state magic-angle-spinning NMR spectroscopy. Nature 420:98–102
Chatelier RC, Minton AP (1987) Sedimentation equilibrium in macromolecular solutions of arbitrary concentration. I. Self-associating proteins. Biopolymers 26:507–524
Cole HBR, Torchia DA (1991) An NMR study of the backbone dynamics of staphylococcal nuclease in the crystalline state. Chem Phys 158:271–281
Concistre M, Johannessen OG, Carignani E, Geppi M, Levitt M (2013) Magic-angle spinning NMR of cold samples. Acc Chem Res. doi:10.1021/ar300323c
Corzilius B, Smith AA, Barnes AB, Luchinat C, Bertini I, Griffin RG (2011) High-filed dynamic nuclear polarization with high spin transition metal ions. J Am Chem Soc 133:5648–5651
Corzilius B, Smith AA, Griffin RG (2012) Solid effect in magic angle spinning dynamic nuclear polarization. J Chem Phys 173:054201
Cross TA, Opella SJ (1983) Protein structure by solid-state NMR. J Am Chem Soc 105:306–308
de la Torre JG, Huertas ML, Carrasco B (2000) Calculation of hydrodynamic properties of globular proteins from their atomic-level structure. Biophys J 78:719–730
Debelouchina GT, Platt GW, Bayro MJ, Radford SE, Griffin RG (2010) Magic angle spinning NMR analysis of beta(2)-microglobulin amyloid fibrils in two distinct morphologies. J Am Chem Soc 132:10414–10423
Denisov VP, Venu K, Peters J, Horlein HD, Halle B (1997) Orientational disorder and entropy of water in protein cavities. J Phys Chem B 101:9380–9389
Diakova G, Goddard YA, Korb J-P, Bryant RG (2010) Water and backbone dynamics in a hydrated protein. Biophys J 98:138–146
Doucette PA, Whitson LJ, Cao X, Schirf V, Demeler B, Valentine JS, Hansen JC, Hart PJ (2004) Dissociation of human copper-zinc superoxide dismutase dimers using chaotrope and reductant. Insights into the molecular basis for dimer stability. J Biol Chem 279:54558–54566
Franks WT, van Rossum B-J, Bardiaux B, Ravera E, Parigi G, Luchinat C, Oschkinat H (2012) In: Bertini I, McGreevy KS, Parigi G (eds) NMR of biomolecules: towards mechanistic systems biology. Wiley-VCH Verlag GmbH & Co. KGaA, Weinheim, pp 376–392
Gardiennet C, Schütz AK, Hunkeler A, Kunert B, Terradot L, Böckmann A, Meier BH (2012) A sedimented sample of a 59 kDa dodecameric helicase yields high-resolution solid-state NMR spectra. Angew Chem Int Ed 51:7855–7858
Gelis I, Vitzthum V, Dhimole N, Caporini MA, Schedlbauer A, Carnevale D, Connell SR, Fucini P, Bodenhausen G (2013) Solid-state NMR enhanced by dynamic nuclear polarization as a

novel tool for ribosome structural biology. J Biomol NMR 56:85–93
Goddard YA, Korb J-P, Bryant RG (2009) Water molecule contributions to proton spin-lattice relaxation in rotationally immobilized proteins. J Magn Reson 199:68–74
Ha Y, Shi D, Small GW, Theil EC, Allewell NM (1999) Crystal structure of bullfrog M ferritin at 2.8 Å resolution: analysis of subunit interactions and the binuclear metal center. J Biol Inorg Chem 4:243–256
Hall DA, Maus DC, Gerfen GJ, Inati SJ, Becerra LR, Dahlquist FW, Griffin RG (1997) Polarizarion-enhanced NMR spectroscopy of biomolecules in frozen solution. Science 276:930–932
Harbison GS, Smith SO, Pardoen JA, Courtin JML, Lugtenburg J, Herzfeld J, Mathies RA, Griffin RG (1985) Solid-state carbon-13 NMR detection of a perturbed 6-s-trans chromophore in bacteriorhodopsin. Biochemistry 24:6955–6962
Havlin RH, Tycko R (2005) Probing site-specific conformational distributions in protein folding with solid-state NMR. Proc Natl Acad Sci USA 102:3284–3289
Hefke F, Bagaria A, Reckel S, Ullrich SJ, Dötsch V, Glaubitz C, Güntert P (2011) Optimization of amino acid type-specific ^{13}C and ^{15}N labeling for the backbone assignment of membrane proteins by solution- and solid-state NMR with the UPLABEL algorithm. J Biomol NMR 49:75–84
Hills BP (1992) The proton exchange cross-relaxation model of water relaxation in biopolymer systems. Mol Phys 76:489–508
Hu KN, Yu HH, Swager TM, Griffin RG (2004) Dynamic nuclear polarization with biradicals. J Am Chem Soc 126:10844–10845
Hu K-N, Bajaj VS, Rosay M, Griffin RG (2007) High-frequency dynamic nuclear polarization using mixtures of TEMPO and trityl radicals. J Chem Phys 126:44512-1–44512-7
Hu K-N, Yau W-M, Tycko R (2010) Detection of a transient intermediate in a rapid protein folding process by solid-state nuclear magnetic resonance. J Am Chem Soc 132:24–25
Huang TH, Bachovchin WW, Griffin RG, Dobson CM (1984) High-resolution nitrogen-15 nuclear magnetic resonance studies of α-lytic protease in solid state. Direct comparison of enzyme structure in solution and solid states. Biochemistry 23:5933–5937
Huang K-Y, Amodeo GA, Tong L, McDermott AE (2011) The structure of human ubiquitin in 2-methyl-2,4-pentanediol: a new conformational switch. Protein Sci 20:630–639
Igumenova TI, McDermott AE, Zilm KW, Martin RW, Paulson EK, Wand AJ (2004a) Assignments of carbon NMR resonances for microcrystalline ubiquitin. J Am Chem Soc 126:6720–6727
Igumenova TI, Wand AJ, McDermott AE (2004b) Assignment of the backbone resonances for microcrystalline ubiquitin. J Am Chem Soc 126:5323–5331
Ivins FJ, Montgomery MG, Smith SJM, Morris-Davies AC, Taylor IA, Rittinger K (2009) NEMO oligomerization and its ubiquitin-binding properties. Biochem J 421:243–251
Jakeman DL, Mitchell DJ, Shuttleworth WA, Evans JNS (1998) Effects of sample preparation conditions on biomolecular solid-state NMR lineshapes. J Biomol NMR 12:417–421
Kantardjieff KA, Rupp B (2003) Matthews coefficient probabilities: improved estimates for unit cell contents of proteins, DNA, and protein-nucleic acid complex crystals. Protein Sci 12:1865–1871
Keniry MA, Rothgeb TM, Smith RL, Gutowsky HS, Oldfield E (1983) NMR studies of amino acids and proteins. Side-chain mobility of methionine in the crystalline amino acid and in crystalline sperm whale (Physeter catodon) myoglobin. Biochemistry 22:1917–1926
Kiihne S, Bryant RG (2000) Protein-bound water molecule counting by resolution of 1H spin-lattice relaxation mechanisms. Biophys J 78:2163–2169
Knight MJ, Webber AL, Pell AJ, Guerry P, Barbet-Massin E, Bertini I, Felli IC, Gonnelli L, Pierattelli R, Emsley L, Lesage A, Hermann T, Pintacuda G (2011) Fast resonance assignment and fold determination of human superoxide dismutase by high-resolution proton-detected solid state MAS NMR spectroscopy. Angew Chem Int Ed 50:11697–11701
Knight MJ, Felli IC, Pierattelli R, Bertini I, Emsley L, Hermann T, Pintacuda G (2012a) Rapid measurement of pseudocontact shifts in metalloproteins by proton-detected solid-state NMR spectroscopy. J Am Chem Soc 134:14730–14733
Knight MJ, Pell AJ, Bertini I, Felli IC, Gonnelli L, Pierattelli R, Hermann T, Emsley L, Pintacuda G (2012b) Structure and backbone dynamics of a microcrystalline metalloprotein by solid-state NMR. Proc Natl Acad Sci USA 109:11095–11100
Knight MJ, Felli IC, Pierattelli R, Emsley L, Pintacuda G (2013) Magic angle spinning NMR of paramagnetic proteins. Acc Chem Res. doi:10.1021/ar300349y
Laage S, Marchetti A, Sein J, Pierattelli R, Sass HJ, Grzesiek S, Lesage A, Pintacuda G, Emsley L (2008) Band-selective 1H–13C cross-polarization in fast MAS solid-state NMR spectroscopy. J Am Chem Soc 130:17216–17217
Laage S, Lesage A, Emsley L, Bertini I, Felli IC, Pierattelli R, Pintacuda G (2009a) Transverse-dephasing optimized homonuclear J-decoupling in solid-state NMR spectroscopy of uniformly 13^C-labeled proteins. J Am Chem Soc 131:10816–10817
Laage S, Sachleben J, Steuernagel S, Pierattelli R, Pintacuda G, Emsley L (2009b) Fast acquisition of multi-dimensional spectra in solid-state NMR enabled by ultra-fast MAS. J Magn Reson 196:133–141
Lee AL, Wand AJ (1999) Assessing potential bias in the determination of rotational correlation times of proteins by NMR relaxation. J Biomol NMR 13:101–112
Lewandowski JR, Sein J, Sass HJ, Grzesiek S, Blackledge M, Emsley L (2010) Measurement of site-specific ^{13}C spin-lattice relaxation in a crystalline protein. J Am Chem Soc 132:8252–8254
Lewandowski JR, Dumez JN, Akbey Ü, Franks WT, Emsley L, Oschkinat H (2011a) Enhanced resolution and coherence lifetimes in the solid-state NMR spectroscopy of perdeuterated proteins under ultrafast magic-angle spinning. J Phys Chem Lett 2:2205–2211
Lewandowski JR, Sass HJ, Grzesiek S, Blackledge M, Emsley L (2011b) Site-specific measurement of slow motions in proteins. J Am Chem Soc 133:16762–16765
Lewandowski JR, Van der Wel PCA, Rigney M, Grigorieff N, Griffin RG (2011c) Structural complexity of a composite amyloid fibril. J Am Chem Soc 133:14686–14698
Libralesso E, Nerinovski K, Parigi G, Turano P (2005) 1H nuclear magnetic relaxation dispersion of Cu, Zn superoxide dismutase in the native and guanidinium-induced unfolded forms. Biochem Biophys Res Commun 328:633–639
Linden AH, Franks WT, Akbey Ü, Lange S, van Rossum B-J, Oschkinat H (2011) Cryogenic temperature effects and resolution upon slow cooling of protein preparations in solid state NMR. J Biomol NMR 51:283–292
Liu Z, Zhang W-P, Xing Q, Ren X, Liu M, Tang C (2012) Noncovalent dimerization of ubiquitin. Angew Chem Int Ed 51:469–472
Loquet A, Giller K, Becker S, Lange A (2010) Supramolecular interactions probed by (13)C-(13)C solid-state NMR spectroscopy. J Am Chem Soc 132:15164–15166
Loquet A, Sgourakis NG, Gupta R, Giller K, Riedel D, Goosmann C, Griesinger C, Kolbe M, Baker D, Becker S, Lange A (2012) Atomic model of the type III secretion system needle. Nature 486:276–279
Loquet A, Habenstein B, Lange A (2013) Structural investigations of molecular machines by solid-state NMR. Acc Chem Res. doi:10.1021/ar300320p

Luchinat C, Parigi G, Ravera E, Rinaldelli M (2012) Solid state NMR crystallography through paramagnetic restraints. J Am Chem Soc 134:5006–5009

Luchinat C, Parigi G, Ravera E (2013) Water and protein dynamics in sedimented systems: a relaxometric investigation. Chem Phys Chem. doi:10.1002/cphc.201300167

Lundh S (1980) Concentrated protein solutions in the analytical ultracentrifuge. J Polym Sci Polym Phys Ed 18:1963–1978

Lundh S (1985) Ultacentrifugation of concentrated biopolymer solutions and effect of ascorbate. Arch Biochem Biophys 241:265–274

Lv G, Kumar A, Giller K, Orcellet ML, Riedel D, Fernandez CO, Becker S, Lange A (2012) Structural comparison of mouse and human α-synuclein amyloid fibrils by solid-state NMR. J Mol Biol 420:99–111

Mainz A, Jehle S, van Rossum BJ, Oschkinat H, Reif B (2009) Large protein complexes with extreme rotational correlation times investigated in solution by magic-angle-spinning NMR spectroscopy. J Am Chem Soc 131:15968–15969

Mainz A, Bardiaux B, Kuppler F, Multhaup G, Felli IC, Pierattelli R, Reif B (2012) Structural and mechanistic implications of metal-binding in the small heat-shock protein αB-crystallin. J Biol Chem 287:1128–1138

Margiolaki I, Wright JP, Wilmanns M, Fitch AN, Pinotsis N (2007) Second SH3 domain of ponsin solved from powder diffraction. J Am Chem Soc 129:11865–11871

Martin RW, Zilm KW (2003) Preparation of protein nanocrystals and their characterization by solid state NMR. J Magn Reson 165:162–174

Matsuki Y, Maly T, Ouari O, Karoui H, Le Moigne F, Rizzato E, Lyubenova S, Herzfeld J, Prisner TF, Tordo P, Griffin RG (2009) Dynamic nuclear polarization with a rigid biradical. Angew Chem Int Ed 121:5096–5100

McDermott A (2009) Structure and dynamics of membrane proteins by magic angle spinning solid-state NMR. Annu Rev Biophys 38:385–403

McDermott AE, Polenova T, Böckmann A, Zilm KW, Paulsen EK, Martin RW, Montelione GT (2000) Partial NMR assignments for uniformly (13C, 15N)-enriched BPTI in the solid state. J Biomol NMR 16:209–219

Minton AP (2007) The effective hard particle model provides a simple, robust, and broadly applicable description of nonideal behavior in concentrated solutions of bovine serum albumin and other nonassociating proteins. J Pharm Sci 96:3466–3469

Murray DT, Das N, Cross TA (2013) Solid state NMR strategy for characterizing native membrane protein structures. Acc Chem Res. doi:10.1021/ar3003442

Ni QZ, Daviso E, Can TV, Markhasin E, Jawla SK, Swager TM, Temkin RJ, Herzfeld J, Griffin RG (2013) High frequency dynamic nuclear polarization. Acc Chem Res. doi:10.1021/ar300348n

Paravastu AK, Leapman RD, Yau WM, Tycko R (2008) Molecular structural basis for polymorphism in Alzheimer's beta-amyloid fibrils. Proc Natl Acad Sci USA 105:18349–18354

Pauli J, van Rossum B, Forster H, de Groot HJ, Oschkinat H (2000) Sample optimization and identification of signal patterns of amino acid side chains in 2D RFDR spectra of the alpha-spectrin SH3 domain. J Magn Reson 143:411–416

Petkova AT, Ishii Y, Balbach JJ, Antzutkin ON, Leapman RD, Delaglio F, Tycko R (2002) A structural model for Alzheimer's beta-amyloid fibrils based on experimental constraints from solid state NMR. Proc Natl Acad Sci USA 99:16742–16747

Pines A, Gibby MG, Waugh JS (1972) Proton-enhanced nuclear induction spectroscopy. A method for high resolution NMR of dilute spins in solids. J Chem Phys 56:1776–1777

Qiang W, Yau W-M, Luo Y, Mattson MP, Tycko R (2012) Antiparallel β-sheet architecture in Iowa-mutant β-amyloid fibrils. Proc Natl Acad Sci USA 109:4443–4448

Ravera E, Corzilius B, Michaelis VK, Rosa C, Griffin RG, Luchinat C, Bertini I (2013a) Dynamic nuclear polarization of sedimented solutes. J Am Chem Soc 135:1641–1644

Ravera E, Parigi G, Mainz A, Religa TL, Reif B, Luchinat C (2013b) Experimental determination of microsecond reorientation correlation times in protein solutions. J Phys Chem B 117:3548–3553

Rivas G, Minton AP (2011) Beyond the second virial coefficient: sedimentation equilibrium in highly non-ideal solutions. Methods 54:167–174

Rothgeb TM, Oldfield E (1981) Nuclear magnetic resonance of heme protein crystals. General aspects. J Biol Chem 256:1432–1446

Salager E, Stein RS, Steuernagel S, Lesage A, Elena B, Emsley L (2009) Enhanced sensitivity in high-resolution 1H solid-state NMR spectroscopy with DUMBO dipolar decoupling under ultra-fastMAS. Chem Phys Lett 469:336–341

Seidel K, Etzkorn M, Heise H, Becker S, Baldus M (2005) High-resolution solid-state NMR studies on uniformly [13C,15N]-labeled ubiquitin. ChemBioChem 6:1638–1647

Sengupta I, Nadaud PS, Jaroniec CP (2013) Protein structure determination with paramagnetic solid-state NMR spectroscopy. Acc Chem Res. doi:10.1021/ar300360q

Sheng Y, Chattopadhyay M, Whitelegge JP, Valentine JS (2012) SOD1 aggregation and ALS: role of metallation states and disulfide status. Curr Top Med Chem 12:2560–2572

Siemer AB, McDermott AE (2008) Solid-state NMR on a type III antifreeze protein in the presence of ice. J Am Chem Soc 130:17394–17399

Siemer AB, Huang K-Y, McDermott AE (2012) Protein linewidth and solvent dynamics in froze solution NMR. PLoS One 7:e47242

Smith SO, Farr-Jones S, Griffin RG, Bachovchin WW (1989) Crystal versus solution structures of enzymes: NMR spectroscopy of a crystalline serine protease. Science 244:961–964

Thurber KR, Tycko R (2008) Biomolecular solid state NMR with magic-angle spinning at 25 K. J Magn Reson 195:179–186

Thurber KR, Tycko R (2009) Measurement of sample temperatures under magic-angle spinning from the chemical shift and spin-lattice relaxation rate of ^{79}Br in KBr powder. J Magn Reson 196:84–87

Turano P, Lalli D, Felli IC, Theil EC, Bertini I (2010) NMR reveals a pathway for iron mineral precursors to the central cavity of ferritin. Proc Natl Acad Sci USA 107:545–550

Tycko R (2011) Solid-state NMR studies of amyloid fibril structure. Annu Rev Phys Chem 62:10–20

Tycko R (2013) NMR at Low and Ultralow Temperatures. Acc Chem Res. doi:10.1021/ar300358z

Van der Wel PC, Hu KN, Lewandowski J, Griffin RG (2006) Dynamic nuclear polarization of amyloidogenic peptide nanocrystals: GNNQQNY, a core segment of the yeast prion protein Sup35p. J Am Chem Soc 128:10840–10846

Van der Wel PC, Lewandowski JR, Griffin RG (2007) Solid-state NMR study of amyloid nanocrystals and fibrils formed by the peptide GNNQQNY from yeast prion protein Sup35p. J Am Chem Soc 129:5117–5130

Venturi L, Woodward N, Hibberd D, Marighedo N, Gravelle A, Ferrante G, Hills BP (2008) Multidimensional cross-correlation relaxometry of aqueous protein systems. Appl Magn Reson 33:213–234

Venu K, Denisov VP, Halle B (1997) Water 1H magnetic relaxation dispersion in protein solutions. A quantitative assessment of internal hydration, proton exchange, and cross-relaxation. J Am Chem Soc 119:3122–3134

Wasmer C, Lange A, Van Melckebeke H, Siemer AB, Riek R, Meier BH (2008) Amyloid fibrils of the HET-s(218-289) prion form a

beta solenoid with a triangular hydrophobic core. Science 319:1523–1526

Webber AL, Pell AJ, Barbet-Massin E, Knight MJ, Bertini I, Felli IC, Pierattelli R, Emsley L, Lesage A, Pintacuda G (2012) Combination of DQ and ZQ coherences for sensitive through-bond NMR correlation experiments in biosolids under ultra-fast MAS. ChemPhysChem 13:2405–2411

Weis V, Griffin RG (2006) Electron-nuclear cross polarization. Solid State Nucl Magn Reson 29:66–78

Yan S, Suiter CL, Hou G, Zhang H, Polenova T (2013) Probing structure and dynamics of protein assemblies by magic angle spinning NMR spectroscopy. Acc Chem Res. doi:10.1021/ar300309s